Published in final edited form as:
Phys Med Biol. 2010 July 7; 55(13): 3859–3871. doi:10.1088/0031-9155/55/13/019.

In vivo real-time rectal wall dosimetry for prostate radiotherapy

Nicholas Hardcastle[1,2], **Dean L. Cutajar**[1], **Peter E. Metcalfe**[1], **Michael L. F. Lerch**[1], **Vladimir L. Perevertaylo**[4], **Wolfgang A. Tomé**[1,2,3], and **Anatoly B. Rosenfeld**[1]

[1] Centre for Medical Radiation Physics, University of Wollongong, Wollongong, NSW, Australia, 2522

[2] Dept. Human Oncology, University of Wisconsin – Madison, 600 Highland Ave, K4/314, Madison, WI, USA, 53792

[3] Dept. Medical Physics, University of Wisconsin – Madison, 600 Highland Ave, K4/314, Madison, WI, USA, 53792

[4] SPA BIT, Kiev, Ukraine

Abstract

Rectal balloons are used in external beam prostate radiotherapy to provide reproducible anatomy and rectal dose reductions. This is an investigation into the combination of a MOSFET radiation detector with a rectal balloon for real time *in vivo* rectal wall dosimetry. The MOSFET used in the study is a radiation detector that provides a water equivalent depth of measurement of 70μm. Two MOSFET*s* were combined in a face-to-face orientation. The reproducibility, sensitivity and angular dependence were measured for the dual MOSFET in a 6MV photon beam. The dual MOSFET was combined with a rectal balloon and irradiated with hypothetical prostate treatments in a phantom. The anterior rectal wall dose was measured in real time and compared with the planning system calculated dose.

The dual MOSFET showed angular dependence within ± 2.5% in the azimuth and +2.5%/-4% in the polar axes. When compared with an ion chamber measurement in a phantom, the dual MOSFET agreed within 2.5% for a range of radiation path lengths and incident angles. The dual MOSFET had reproducible sensitivity for fraction sizes of 2-10Gy. For the hypothetical prostate treatments the measured anterior rectal wall dose was 2.6% and 3.2% lower than the calculated dose for 3DCRT and IMRT plans. This was expected due to limitations of the dose calculation method used at the balloon cavity interface.

A dual MOSFET combined with a commercial rectal balloon was shown to provide reproducible measurements of the anterior rectal wall dose in real time. The measured anterior rectal wall dose agreed with the expected dose from the treatment plan for 3DCRT and IMRT plans. The dual MOSFET could be read out in real time during the irradiation, providing capability for real time dose monitoring of the rectal wall dose during treatment.

Keywords

mosfet; in vivo; rectal wall; prostate; rectal balloon

Corresponding Author: Nicholas Hardcastle – nick.hardcastle@gmail.com & Anatoly Rosenfeld – anatoly@uow.edu.au.

*Author #1 is now at the University of Wisconsin – Madison. The address is as per institution #2.

Introduction

Modern external beam radiotherapy for prostate cancer involves the delivery of high doses using highly conformal delivery techniques. Increased prostate dose has been shown to increase local control. (Hanks et al., 1998, Pollack et al., 2000, Zelefsky et al., 1998) Additionally, hypofractionation has been shown to be an attractive delivery method due to the apparent low alpha/beta ratio for the prostate. (Brenner and Hall, 1999, Brenner et al., 2002, Fowler et al., 2001) Increasing the total treatment dose or the dose per fraction increases the need for accurate delivery verification.

In vivo dosimetry of the rectal wall is an appealing method for verification of target and organ at risk (OAR) doses. An *in vivo* dosimeter placed on the anterior rectal wall would allow the clinician to measure the dose delivered to the section of the rectum receiving the highest dose. This is important, particularly for recent hypofractionation schedules, where high doses are delivered to the prostate and anterior rectal wall, and would be particularly useful in the context of the limitations of dose calculation algorithms at cavity interfaces. (Hardcastle et al., 2009, Keall and Hoban, 1996, Martens et al., 2002) Additionally, accurate knowledge of the anterior rectal wall dose is necessary for correlation of delivered dose to rectal toxicity. A secondary application of an *in vivo* anterior rectal wall dosimeter would be for target dose verification. The anterior rectal wall is generally contained by the Planning Target Volume (PTV) therefore any dosimeter placed on the anterior rectal wall can be used as a surrogate for the PTV dose at the posterior region of the volume.

Recent articles have focused on implantable *in vivo* dosimeters for target dose verification. (Beyer et al., 2007, Black et al., 2005, Fagerstrom et al., 2008, Kry et al., 2009, Scarantino et al., 2008, Scarantino et al., 2005) This is a useful method of *in vivo* dose verification for prostate radiotherapy, with the added advantage that the implanted dosimeter can be used for position verification. (Kry et al., 2009) Other methods have focused on placing a dosimeter in a urethral catheter, for *in vivo* verification of the prostate dose in brachytherapy. (Bloemen-van Gurp et al., Bloemen-van Gurp et al., 2009, Cygler et al., 2006, Soriani et al., 2007) Yet another tool for *in vivo* prostate dosimetry is the Electronic Portal Imaging Device (EPID). Various studies have been presented that investigate using the EPID to measure transmitted fluence and then using this measured fluence to calculate the the dose delivered to the patient. These methods are summarized by van Elmpt et. al.. (van Elmpt, 2008)

This phantom study investigates another method of *in vivo* dosimetry for prostate radiotherapy using rectal balloons. Rectal balloons are used in a number of institutions in prostate radiotherapy to immobilise the prostate and reduce the amount of rectal wall irradiated to high doses. (McGary et al., 2002, Patel et al., 2003, Teh et al., 2005, Teh et al., 2002, van Lin et al., 2005a, van Lin et al., 2007, van Lin et al., 2005b, Wachter et al., 2002) Rectal balloons are placed in the rectum for each treatment fraction. Rectal balloons provide an excellent means for placement of an *in vivo* dosimeter. In this report, the utility of a commercial rectal balloon in combination with a MOSFET detector for real-time *in vivo* dose measurements at the rectal wall is examined. Real-time rectal wall measurements were carried out on a specially designed phantom in conventional external beam radiotherapy scenarios.

Methods and materials

MOSFET Detectors

MOSFET detectors have been used extensively for *in vivo* dosimetry. (Butson et al., 1996, Quach et al., 2000, Scalchi and Francescon, 1998, Scalchi et al., 2005, Zilio et al., 2006) The advantages of the MOSFET dosimetry system for point dose measurements are their

relatively small size and real-time readout capabilities. (Kron et al., 2002, Rosenfeld et al., 2001) MOSFET dosimetry relies on ionizing radiation altering the electrical properties of the MOSFET, specifically the threshold voltage (V_t), for a given source-drain current. The change in V_t is proportional to the absorbed dose. A MOSFET detector developed at CMRP (known as the 'MO*Skin*') was used for all measurements. This specific MOSFET detector has been described in detail elsewhere and has been used extensively for *in vivo* measurements. (Hardcastle et al., 2008, Kwan et al., 2008a, Kwan et al., Kwan et al., 2009, Qi et al., 2009) In summary, this MOSFET has reproducible Water Equivalent Depth (WED) of measurement of 70μm with a sensitive volume defined by the volume of the gate oxide of $4.8 \times 10^{-6} mm^3$. This makes the design of the MOSFET ideal for dosimetry in high dose gradient regions, such as the rectal wall in the presence of a rectal balloon air cavity.

In the case of measurements at depth (rather than at the surface), two MOSFET*s* are used, in a face to face arrangement. This face to face dual MOSFET arrangement is referred to in the remainder of this text as the 'dual MOSFET'. The dual MOSFET, proposed and developed at CMRP, allows for angular independent measurements as it negates the naturally asymmetrical structure of the MOSFET chip relative to the beam direction. (Rosenfeld et al., 2005) It must be stated that this definition of the dual MOSFET is functionally different to commercial dual MOSFET detectors, where two MOSFET chips on the same Si substrate are used for temperature compensation. (Soubra et al., 1994) In our case, the dual MOSFET relates to correction of angular anisotropy and not temperature compensation. The dual MOSFET results in a dose measurement effectively made over a 140μm thick region. The dual MOSFET was embedded into the outer lumen of a commercial rectal balloon (RadiaDyne, Houston TX, USA), as shown in Figure 1, such that it is fully contained within the balloon.

The MOSFET detectors are read out in real time using an in-house developed reader. The reader provides a 15V gate voltage to the MOSFET during irradiation. The reader then supplies a constant source-drain current to deduce V_t. The reader can be used to read out V_t manually or can be controlled by a PC for automatic read out over a given time interval at a set frequency using in-house developed software. (Rosenfeld et al., 2001)

Reproducibility and Sensitivity

The reproducibility of the sensitivity of the MOSFET detector, that is, the change in V_t for irradiation to known doses, was measured. The sensitivity was investigated for a range of simulated treatment fraction deliveries from 2-10Gy/fraction, including simulated breaks for gantry motion between beams. The rectal balloons are designed for one fraction use only; each balloon/MOSFET would receive only one fraction of dose. The MOSFET*s* were irradiated at 1.5cm depth in a $30\times30\times=11.5cm^3$ water slab with a $10\times10cm^2$ 6MV photon beam at 100cm SSD. Seven field treatment fractions of 2-10Gy/fraction were simulated by irradiating a MOSFET up to the fraction dose in seven equal increments (to simulate irradiation from each 'beam'). A delay of 30s was used in between each 'beam' to simulate time for gantry rotation between beams. A new MOSFET with no dose history was used for each simulated fraction. The fraction sizes simulated are given in Table 1.

Angular Dependence

The angular dependence of the dual MOSFET configuration was measured in two axes in a 6MV photon beam from a Varian 21EX LINAC. The angular dependence in the azimuth axis was measured by placing the dual MOSFET in a cylindrical phantom that was embedded in a square, solid water phantom at a depth of 5cm. The dual MOSFET was then irradiated from a beam incident every 30° for a full rotation. This was repeated twice. The cylinder containing the dual MOSFET was rotated, rather than the LINAC gantry, to

maintain constant radiation path length to the location of the detector. The polar angular dependence was measured by placing the dual MOSFET in the centre of a 10cm diameter cylinder, orthogonal to the cylinder's longitudinal axis. The dual MOSFET was irradiated with a $5\times5cm^2$ field in increments of 30° around the full 360° of the cylinder. For each measurement, the average response of the two detectors was then taken as the final reading. All readings were normalized to the average of the measurements at each angle for each measurement axis.

A further set of measurements with the dual MOSFET was performed to measure the angular dependence at different depths using a clinical IMRT verification phantom - I'mRT (IBA Dosimetry). The dual MOSFET was placed at the centre of the phantom and calibrated. Calibration was performed by irradiating the dual MOSFET with a known dose and recording the response of both detectors. The dual MOSFET was then flipped and the calibration was repeated. For each calibration measurement the change in threshold voltage for each detector was added. The average of the responses (i.e. in both orientations) was then divided by the known dose (100cGy) to give the MOSFET sensitivity in mV/cGy. The calibration coefficient is the inverse of the sensitivity and has the units of cGy/mV. The voltage reading is multiplied by the calibration coefficient to obtain the dose.

The dual MOSFET was then irradiated from gantry angles every 45°for the full 360° (detector was at machine isocentre). Each measurement was multiplied by the dual MOSFET calibration coefficient to result in absolute dose for each measurement. The dual MOSFET was then replaced with the ion chamber. The ion chamber was calibrated by irradiating with a known dose. The ion chamber was then irradiated with the same gantry angles as for the dual MOSFET. The dual MOSFET dose was normalized to the ion chamber measurement at each angle. All measurements were repeated twice.

Treatment Simulation Measurements

A custom made phantom was built to match the external contours of the balloon. This phantom was placed in the I'mRT phantom. The phantom set up is shown in Figure 2. A planning CT scan was taken of the phantom set up. The CT data was transferred into the Pinnacle RTPS (Philips Medical Systems, Middleton, WI, USA) where contours of a hypothetical prostate, rectum (the balloon cavity), bladder and femoral heads were created. Seven field 3DCRT and IMRT plans were created in the Pinnacle RTPS, delivering 78Gy in 2Gy fractions to the isocentre of a hypothetical prostate target in the phantom. The MOSFET was visible on the CT scan (Figure 2c) and the planned dose to the MOSFET was recorded for both treatment plans. Three fractions each of the 3DCRT and IMRT plans were then delivered to the phantom.

The dose delivered to the dual MOSFET was recorded at a frequency of 1Hz during each delivery using connection of the reader to a PC and in-house developed software. The dual MOSFET was irradiated in active mode, meaning a bias voltage was applied to the gate oxide during irradiation to increase sensitivity. During readout, the gate voltage is inverted and the threshold voltage is obtained for a given readout current. As the gate voltage of the MOSFET is inverted during this read out, the charge collection in the active volume hence the sensitivity is affected. However, the read out of the MOSFET, controlled by a microprocessor, takes approximately 100μs or 0.01% of the duty cycle meaning this effect is negligible.

Results

Reproducibility

The sensitivity of seven MOSFET detectors from the same batch for irradiation for fraction sizes of 2Gy up to 10Gy (each 'fraction' irradiated in seven increments) is presented in Table 1. The response of the seven MOSFET detectors was on average (± standard deviation) 2.63 ± 0.01 mV/cGy.

Angular Dependence

The angular dependence of the dual MOSFET is presented in Figure 3. The results are the average of three measurements and the error bars are two standard deviations of the mean. The variation in readings for the azimuth axis was within ± 2.5%. For the polar axis the readings are between -2.5% and +4% of the average of all readings.

The dual MOSFET measured dose, relative to the ion chamber measurement at the centre of the I'mRT phantom for beams incident from various angles is given in Figure 4. The dual MOSFET measured dose at the centre of the I'mRT phantom was within ±2.5% of the ion chamber measured dose at the same location.

Treatment Simulation Measurements

The dual MOSFET real-time measured dose, at the anterior rectal wall in a phantom set up is presented in Figure 5. The error bars are the 95% confidence interval of the average of three measurements. For the 3DCRT plan, the dual MOSFET measured dose was 184.5 ± 0.8cGy and the RTPS calculated dose was 189.4cGy. This is a difference of -5.1cGy, or the dual MOSFET measured dose is 2.6% lower than the planned dose. For the IMRT plan, the influence of the segmented dose delivery is apparent in the more jagged shape of the real-time dose accrual plot. The dual MOSFET measured dose was 185.1 ± 1.3cGy and the RTPS calculated dose was 191.2cGy. This is a difference of 6.1cGy, or the dual MOSFET measured dose is 3.2% lower than the planned dose.

The RTPS calculated dose for each field was compared with the dual MOSFET measured dose for each field for the 3DCRT and IMRT treatment deliveries. Figure 6 shows the comparison between the planned and measured rectal wall dose. For the 3DCRT plan, the dual MOSFET measured doses agree, within error limits, with the RTPS calculated dose for the 120°, 40°, 0°, 320° beams. For the 80°, 240° and 280° beams, the RTPS is 1.0 cGy, 1.4 cGy and 3.2cGy more than the dual MOSFET measured dose respectively. For the IMRT plan, the dual MOSFET measured doses agree within error limits with the RTPS calculated dose for the 40°, 0° and 320° beams. For the 120°, 80°, 240° and 280° beams, the RTPS calculated dose is 2.3cGy, 1.5cGy, 0.7cGy and 1.25cGy greater than the dual MOSFET measured doses respectively.

Discussion

This study has presented initial results from testing of a MOSFET dosimeter developed at the CMRP combined with a rectal balloon for use in real-time *in vivo* dosimetry. In this phantom study, the performance of a dual MOSFET configuration in combination with a commercial rectal balloon was investigated to determine the utility of this apparatus for clinical use.

The MOSFET detectors showed a reproducible sensitivity for fraction sizes of 2-10Gy. The very good reproducibility of the MOSFET sensitivity (within 1%) is related to the low dose exposures up to 10Gy, where there is limited radiation damage to the SiO - Si interface.

Thus, the instability of the MOSFET reading is limited. In addition, this comparison was only performed for MOSFETs from the same manufacturing batch. For higher doses, the reproducibility of the sensitivity of MOSFETs is approximately 2% and should be investigated in the future for multiple batches of these particular MOSFETs. This MOSFET is thus suitable for *in vivo* real-time dose monitoring in hypofractionation schedules of up to 10Gy/fraction, such as those seen in prostate cancer radiotherapy. Although the lifetime of the MOSFET is limited to approximately 50Gy, commercial rectal balloons are designed for one use only therefore it is expected that both the balloon and the MOSFET will be discarded after each fraction has been delivered, which for prostate radiotherapy would typically by less than 10Gy.

The dual MOSFET has an angular dependence of ± 2.5% from all incident beam angles. Therefore it can be used in rotational therapies such as tomotherapy and volumetric modulated arc therapy (VMAT) without need for angular correction.

When placed on the anterior wall of a commercial rectal balloon and irradiated with clinical 3DCRT and IMRT plans, the dual MOSFET provided real-time dose measurement of the anterior rectal wall dose. The anterior rectal wall dose was measured to be 2.6% and 3.2% lower than the RTPS calculation for the 3DCRT and IMRT plans respectively. Previous studies have shown that the collapsed cone convolution/superposition dose calculation algorithm used in this study over-predicts the anterior rectal wall dose when an air-filled rectal balloon is used. (Hardcastle et al., 2009) Therefore the lower measured dose, relative to the RTPS calculation, concurs with this previous finding.

In Figure 6 it is shown that the dual MOSFET measured doses agree with the RTPS calculated doses for the 320°, 0° and 40° beams for both the 3DCRT and IMRT cases. The RTPS calculated doses were greater than the dual MOSFET measured doses for the 120° (IMRT only), 80°, 280° and 240° beams. These beams deliver dose to the target from beam angles that are more tangential to the target with respect to the balloon cavity. Although the absolute value of the differences were small, this agrees with a previous study that showed the greatest discrepancy between the RTPS calculated dose and the measured dose at the anterior rectal wall in the presence of a rectal balloon cavity was when the beams were incident laterally to the target, with respect to the cavity. (Hardcastle et al., 2009) This is due to limitations in the convolution/superposition dose calculation where lateral electron disequilibrium exists. Therefore any differences between the RTPS calculated and measured doses at the anterior rectal wall when an air-filled rectal balloon is used would be expected to be due mainly to the contribution from lateral beams.

The MOSFET was able to be read out at 1Hz during the delivery of a radiotherapy treatment fraction. The ability to read out the MOSFET in real-time allows the rectal dose to be tracked as it is being delivered, potentially providing a ‘dose alarm’ if the rectal wall dose exceeds a set tolerance. This has been shown in the results in Figure 6; the tracking of the anterior rectal wall dose can be performed on a field-by-field basis. Although the rectal balloon reduces prostate motion significantly, rectal motion can still occur which may increase rectal wall dose. Conversely, if the rectal wall dose is significantly lower than the expected dose this could mean part of the PTV is being underdosed. At the very least, this *in vivo* dosimetry system provides tracking and verification of daily delivered rectal wall doses, which may prove useful in the case of observed enhancement of toxicity or local recurrence. Correlation of rectal toxicity rates with absorbed dose currently relies on calculated dose at the time of planning. This device would provide a direct measurement of the anterior rectal wall dose for each treatment fraction, increasing the accuracy of toxicity correlation.

Use of this *in vivo* detector system will become more complicated when used in clinical patients. Complications may arise due to any temperature changes of the MOSFET during irradiation and balloon positioning in the patient. These complications must be taken into account to ensure accurate dosimetry.

The threshold voltage of the MOSFET detectors is sensitive to temperature variations unless the readout current corresponds to the thermostable current, as used in the current reader. The thermostable current is the readout current (source-drain current) at which the threshold voltage is constant for varying temperature. The thermostable current is constant for the dose range presented in this paper. Sensitivity to radiation of the MOSFET detector is temperature independent within (15°-40°). (Cheung T, 2004) Thus calibration made at any room temperature, if held constant during the calibration process, will be valid for irradiation in different temperatures, for example 37° on a patient body assuming the MOSFET temperature is constant during real-time dosimetry. However, the threshold voltage of the MOSFET changes with temperature. (Cheung T, 2004) Therefore, In order to avoid temperature error associated with transition time where the MOSFET detector is placed on the patient's body, but does not have enough time to obtain thermal equilibrium before measurements commence, the threshold voltage reading of the MOSFET detector should be temperature independent or compensated for. This has been achieved in other MOSFET detections systems using a dual MOSFET with different gate bias during irradiation. (Soubra et al., 1994) The next generation CMRP read out system for MOSFET detectors and dual MOSFET detectors is temperature independent for any readout current without requiring an additional MOSFET chip. This system utilizes the intrinsic properties of MOSFET detectors for real-time correction of temperature changes without the need for additional temperature sensors. (Rozenfeld, 2008)

A second complication arises in balloon/detector positioning. Currently the balloon has markings on the stem which help to ensure the correct depth of insertion during simulation and delivery of the treatment. During the treatment, detector localization accuracy would depend on the level of image guidance being employed. As shown in Figure 2c, the MOSFET is visible on the planning CT. Therefore, kilovoltage CT image data taken immediately prior to treatment delivery would provide accurate detector location for this snapshot of time. In this case, the dose could be recalculated to obtain the expected daily dose for comparison with the measured dose, integrating with any image guidance or adaptive protocols. If this level of image guidance is not employed, then the MOSFET location would not as accurately be known in the face of anatomical changes. In the case of variation in balloon positioning between fractions, a future design could employ multiple dual MOSFET detectors placed in a strip along the superior-inferior axis of the balloon. This would provide dose measurement at multiple locations along the anterior rectal wall relative to the PTV and improve the probability of measurement of the highest anterior rectal wall dose. In addition to anterior rectal wall dose measurements, MOSFET detectors could be placed at other locations around the balloon, such as the posterior side, to obtain more absorbed dose to the rectum data.

Conclusion

A real-time *in vivo* dosimetry system for tracking of rectal wall doses in prostate radiotherapy has been presented. The dosimetry system provides real time tracking of the rectal wall dose during the delivery of a treatment fraction. The MOSFET detectors provided reproducible, angular independent dose measurements and linear response for fraction sizes of 2-10Gy. A dual MOSFET configuration was used in a phantom set up to measure in real-time the anterior rectal wall dose for 3DCRT and IMRT treatments

(delivering 2Gy/fraction). The measured anterior rectal wall doses were in close agreement with the RTPS calculation and consistent with previous dosimetry studies in this situation.

Acknowledgments

The authors would like to thank Iolanda Fuduli and Peter Ihnat for assistance with MOSFET probe construction and Dr. Martin Carolan for assistance with experiments. The authors would also like to thank Australian Rotary Health, the NSW Cancer Institute Clinical Leaders and United States National Institute of Health R01-CA106835 funding assistance for this research (NH, PEM & WAT respectively). The authors acknowledge a commercial licensing agreement with RadiaDyne.

References

Beyer GP, Scarantino CW, Prestidge BR, Sadeghi AG, Anscher MS, Miften M, Carrea TB, Sims M, Black RD. Technical Evaluation of Radiation Dose Delivered in Prostate Cancer Patients as Measured by an Implantable MOSFET Dosimeter. International Journal of Radiation Oncology*Biology*Physics. 2007; 69:925–935.

Black RD, Scarantino CW, Mann GG, Anscher MS, Ornitz RD, Nelms BE. An analysis of an implantable dosimeter system for external beam therapy. International Journal of Radiation Oncology*Biology*Physics. 2005; 63:290–300.

Bloemen-Van Gurp EJ, Haanstra BKC, Murrer LHP, Van Gils FCJM, Dekker ALAJ, Mijnheer BJ, Lambin P. In Vivo Dosimetry with a Linear MOSFET Array to Evaluate the Urethra Dose during Permanent Implant Brachytherapy Using Iodine-125. International Journal of Radiation Oncology*Biology*Physics. In Press, Corrected Proof.

Bloemen-Van Gurp EJ, Murrer LHP, Haanstra BKC, Van Gils FCJM, Dekker ALAJ, Mijnheer BJ, Lambin P. In Vivo Dosimetry Using a Linear Mosfet-Array Dosimeter to Determine the Urethra Dose In 125I Permanent Prostate Implants. International Journal of Radiation Oncology*Biology*Physics. 2009; 73:314–321.

Brenner DJ, Hall EJ. Fractionation and protraction for radiotherapy of prostate carcinoma. Int J Radiat Oncol Biol Phys. 1999; 43:1095–101. [PubMed: 10192361]

Brenner DJ, Martinez AA, Edmundson GK, Mitchell C, Thames HD, Armour EP. Direct evidence that prostate tumors show high sensitivity to fractionation (low alpha/beta ratio), similar to late-responding normal tissue. Int J Radiat Oncol Biol Phys. 2002; 52:6–13. [PubMed: 11777617]

Butson MJ, Rozenfeld A, Mathur JN, Carolan M, Wong TPY, Metcalfe PE. A new radiotherapy surface dose detector: The MOSFET. Medical Physics. 1996; 23:655–658. [PubMed: 8724737]

Cheung T,BM, Pkn Yu. Effects of temperature variation on MOSFET dosimetry. Physics in Medicine and Biology. 2004; 49:N191–N196. [PubMed: 15285264]

Cygler JE, Saoudi A, Perry G, Morash C, E C. Feasibility study of using MOSFET detectors for in vivo dosimetry during permanent low-dose-rate prostate implants. Radiotherapy And Oncology. 2006; 80:296–301. [PubMed: 16905209]

Fagerstrom JM, Micka JA, Dewerd LA. Response of an implantable MOSFET dosimeter to Ir-192 HDR radiation. Medical Physics. 2008; 35:5729–5737. [PubMed: 19175130]

Fowler J, Chappell R, Ritter M. Is alpha/beta for prostate tumors really low? Int J Radiat Oncol Biol Phys. 2001; 50:1021–31. [PubMed: 11429230]

Hanks GE, Hanlon AL, Schultheiss TE, Pinover WH, Movsas B, Epstein BE, Hunt MA. Dose escalation with 3D conformal treatment: five year outcomes, treatment optimization, and future directions. Int J Radiat Oncol Biol Phys. 1998; 41:501–10. [PubMed: 9635695]

Hardcastle N, Metcalfe PE, Rosenfeld AB, Tome WA. Endo-rectal balloon cavity dosimetry in a phantom: Performance under IMRT and helical tomotherapy beams. Radiotherapy And Oncology. 2009; 92:48–56. [PubMed: 19339071]

Hardcastle N, Soisson E, Metcalfe P, Rosenfeld AB, Tome WA. Dosimetric verification of helical tomotherapy for total scalp irradiation. Medical Physics. 2008; 35:5061–5068. [PubMed: 19070240]

Keall PJ, Hoban PW. Superposition dose calculation incorporating Monte Carlo generated electron track kernels. Med Phys. 1996; 23:479–85. [PubMed: 9157258]

Kron T, Rosenfeld A, Lerch M, Bazley S. Measurements in radiotherapy beams using on-line mosfet detectors. Radiation Protection Dosimetry. 2002; 101:445–448. [PubMed: 12382787]

Kry SF, Price M, Wang Z, Mourtada F, Salehpour M. Investigation into the use of a MOSFET dosimeter as an implantable fiducial marker. Journal of Applied Clinical Medical Physics. 2009; 10:22–32.

Kwan IS, Lee B, Yoo AJ, Cho D, Jang K, Shin S, Carolan M, Lerch M, Perevertaylo VL, Rosenfeld AB. Comparison of the New MOSkin Detector and Fiber Optic Dosimetry System for Radiotherapy. Journal of Nuclear Science and Technology. 2008a; S5:518–521. Japan.

Kwan IS, Rosenfeld AB, Qi ZY, Wilkinson D, Lerch MLF, Cutajar DL, Safavi-Naeni M, Butson M, Bucci JA, Chin Y, Perevertaylo VL. Skin dosimetry with new MOSFET detectors. Radiation Measurements. 2008b; 43:929–932.

Kwan IS, Wilkinson D, Cutajar D, Lerch M, Rosenfeld A, Howie A, Bucci J, Chin Y, Perevertaylo VL. The effect of rectal heterogeneity on wall dose in high dose rate brachytherapy. Medical Physics. 2009; 36:224–232. [PubMed: 19235390]

Martens C, Reynaert N, De Wagter C, Nilsson P, Coghe M, Palmans H, Thierens H, De Neve W. Underdosage of the upper-airway mucosa for small fields as used in intensity-modulated radiation therapy: a comparison between radiochromic film measurements, Monte Carlo simulations, and collapsed cone convolution calculations. Med Phys. 2002; 29:1528–35. [PubMed: 12148735]

Mcgary JE, Teh BS, Butler EB, Grant W 3rd. Prostate immobilization using a rectal balloon. J Appl Clin Med Phys. 2002; 3:6–11. [PubMed: 11817999]

Patel RR, Orton N, Tome WA, Chappell R, Ritter MA. Rectal dose sparing with a balloon catheter and ultrasound localization in conformal radiation therapy for prostate cancer. Radiother Oncol. 2003; 67:285–94. [PubMed: 12865176]

Pollack A, Zagars GK, Smith LG, Lee JJ, Von Eschenbach AC, Antolak JA, Starkschall G, Rosen I. Preliminary results of a randomized radiotherapy dose-escalation study comparing 70 Gy with 78 Gy for prostate cancer. J Clin Oncol. 2000; 18:3904–11. [PubMed: 11099319]

Qi Z-Y, Deng X-W, Huang S-M, Zhang L, He Z-C, Li XA, Kwan I, Lerch M, Cutajar D, Metcalfe P, Rosenfeld A. In vivo verification of superficial dose for head and neck treatments using intensity-modulated techniques. Medical Physics. 2009; 36:59–70. [PubMed: 19235374]

Quach KY, Morales J, Butson MJ, Rosenfeld AB, Metcalfe PE. Measurement of radiotherapy x-ray skin dose on a chest wall phantom. Medical Physics. 2000; 27:1676–1680. [PubMed: 10947272]

Rosenfeld AB, Lerch MLF, Kron T, Brauer-Krisch E, Bravin A, Holmes-Siedle A. Feasibility study of on-line, high spatial resolution MOSFET dosimetry in static and pulsed X-ray radiation fields. IEEE Trans. on Nucl.Sci. 2001; NS-48:2061–2068.

Rosenfeld AB, Siegbahn EA, Brauer-Krish E, Holmes-Siedle A, Lerch MLF, Bravin A, Cornelius IM, Takacs GJ, Painuly N, Nettelback H, Kron T. Edge-on face-to-face MOSFET for synchrotron microbeam dosimetry: MC modeling. IEEE Transactions on Nuclear Science. 2005; NS-52:2562–2569.

Rozenfeld AB. Radiation Sensor and Dosimeter. 2008 Australia patent application.

Scalchi P, Francescon P. Calibration of a mosfet detection system for 6-MV in vivo dosimetry. Int J Radiat Oncol Biol Phys. 1998; 40:987–93. [PubMed: 9531385]

Scalchi P, Francescon P, Rajaguru P. Characterization of a new MOSFET detector configuration for in vivo skin dosimetry. Med Phys. 2005; 32:1571–8. [PubMed: 16013716]

Scarantino CW, Prestidge BR, Anscher MS, Ferree CR, Kearns WT, Black RD, Bolick NG, Beyer GP. The Observed Variance Between Predicted and Measured Radiation Dose in Breast and Prostate Patients Utilizing an In Vivo Dosimeter. International Journal of Radiation Oncology*Biology*Physics. 2008; 72:597–604.

Scarantino CW, Rini CJ, Aquino M, Carrea TB, Ornitz RD, Anscher MS, Black RD. Initial clinical results of an in vivo dosimeter during external beam radiation therapy. International Journal of Radiation Oncology*Biology*Physics. 2005; 62:606–613.

Soriani A, Landoni V, Marzi S, Laccarino G, Saracino B, Arcangeli G, Benassi M. Setup verification and in vivo dosimetry during intraoperative radiation therapy (IORT) for prostate cancer. Medical Physics. 2007; 34:3205–3210. [PubMed: 17879783]

Soubra M, Cygler J, Mackay G. Evaluation of a dual bias dual metal oxide-silicon semiconductor field effect transistor detector as radiation dosimeter. Medical Physics. 1994; 21:567–572. [PubMed: 8058024]

Teh BS, Dong L, Mcgary JE, Mai WY, Grant W 3rd, Butler EB. Rectal wall sparing by dosimetric effect of rectal balloon used during intensity-modulated radiation therapy (IMRT) for prostate cancer. Med Dosim. 2005; 30:25–30. [PubMed: 15749008]

Teh BS, Mcgary JE, Dong L, Mai WY, Carpenter LS, Lu HH, Chiu JK, Woo SY, Grant WH, Butler EB. The use of rectal balloon during the delivery of intensity modulated radiotherapy (IMRT) for prostate cancer: more than just a prostate gland immobilization device? Cancer J. 2002; 8:476–83. [PubMed: 12500857]

Van Elmpt WM, Leah, Nijsten Sebastiaan, Wendling Markus, Lambin Philippe, Mijnheer Ben. A literature review of electronic portal imaging for radiotherapy dosimetry. Radiotherapy and Oncology. 2008; 88:289–309. [PubMed: 18706727]

Van Lin EN, Hoffmann AL, Van Kollenburg P, Leer JW, Visser AG. Rectal wall sparing effect of three different endorectal balloons in 3D conformal and IMRT prostate radiotherapy. Int J Radiat Oncol Biol Phys. 2005a; 63:565–76. [PubMed: 16168848]

Van Lin EN, Kristinsson J, Philippens ME, De Jong DJ, Van Der Vight LP, Kaanders JH, Leer JW, Visser AG. Reduced late rectal mucosal changes after prostate three-dimensional conformal radiotherapy with endorectal balloon as observed in repeated endoscopy. Int J Radiat Oncol Biol Phys. 2007; 67:799–811. [PubMed: 17161552]

Van Lin EN, Van Der Vight LP, Witjes JA, Huisman HJ, Leer JW, Visser AG. The effect of an endorectal balloon and off-line correction on the interfraction systematic and random prostate position variations: a comparative study. Int J Radiat Oncol Biol Phys. 2005b; 61:278–88. [PubMed: 15629621]

Wachter S, Gerstner N, Dorner D, Goldner G, Colotto A, Wambersie A, Potter R. The influence of a rectal balloon tube as internal immobilization device on variations of volumes and dose-volume histograms during treatment course of conformal radiotherapy for prostate cancer. Int J Radiat Oncol Biol Phys. 2002; 52:91–100. [PubMed: 11777626]

Zelefsky MJ, Leibel SA, Gaudin PB, Kutcher GJ, Fleshner NE, Venkatramen ES, Reuter VE, Fair WR, Ling CC, Fuks Z. Dose escalation with three-dimensional conformal radiation therapy affects the outcome in prostate cancer. Int J Radiat Oncol Biol Phys. 1998; 41:491–500. [PubMed: 9635694]

Zilio, V.; Joneja, O.; Popowski, Y.; Rosenfeld, A.; Chawla, R. Calibration of MOSFET detectors for absolute dosimetry with an (IR)-I-192 HDR brachytherapy source.. 10th Annual Meeting of the Scientific-Association-of-Swiss-Radiation-Oncology; Sion, SWITZERLAND. 2006. p. 175-175.Year

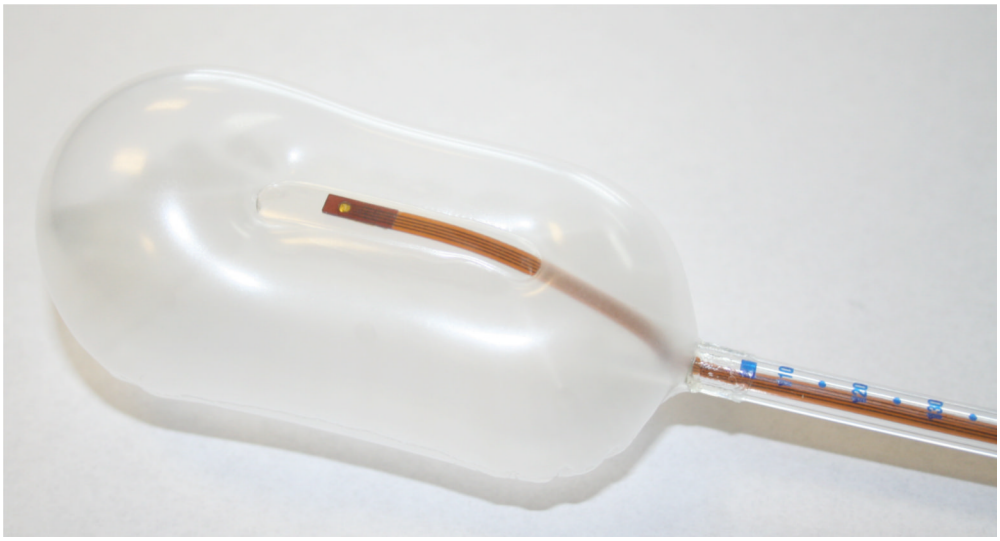

Figure 1.
MOSFET detectors placed in the outer lumen of the RadiaDyne rectal balloon

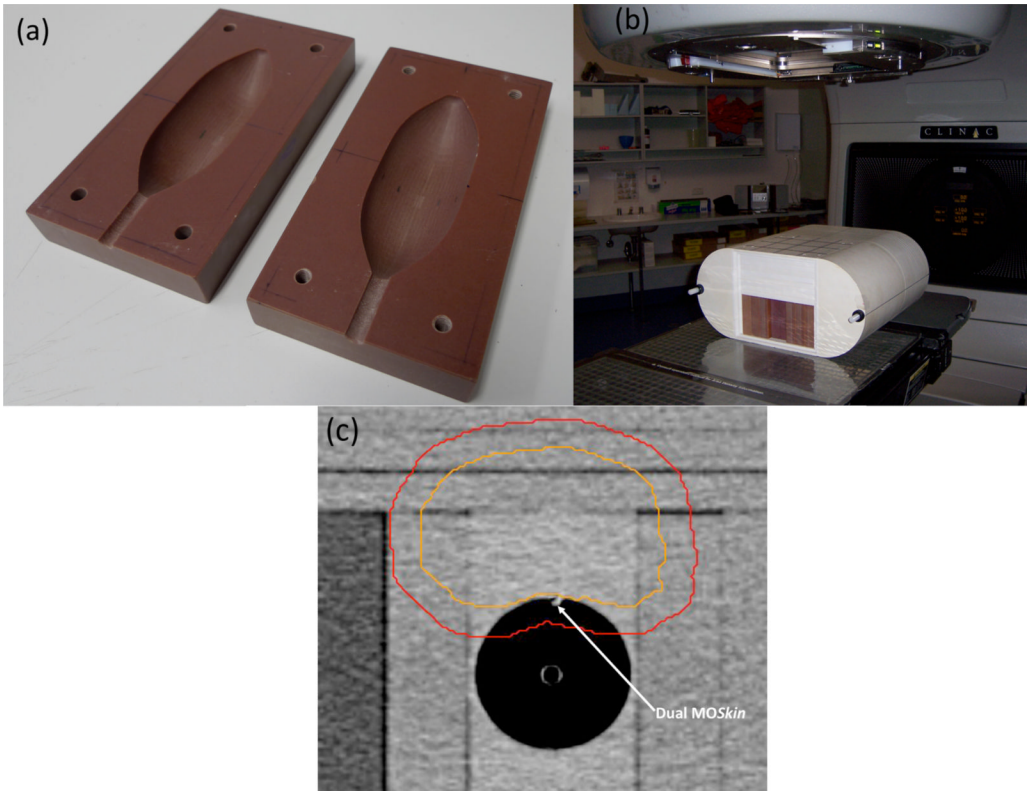

Figure 2.
(a) Custom made phantom to house the rectal balloon (b) Balloon phantom placed inside the I'mRT phantom and (c) CT slice of the phantom showing the dual MOSFET location relative to the hypothetical prostate (inner contour) and PTV (outer contour)

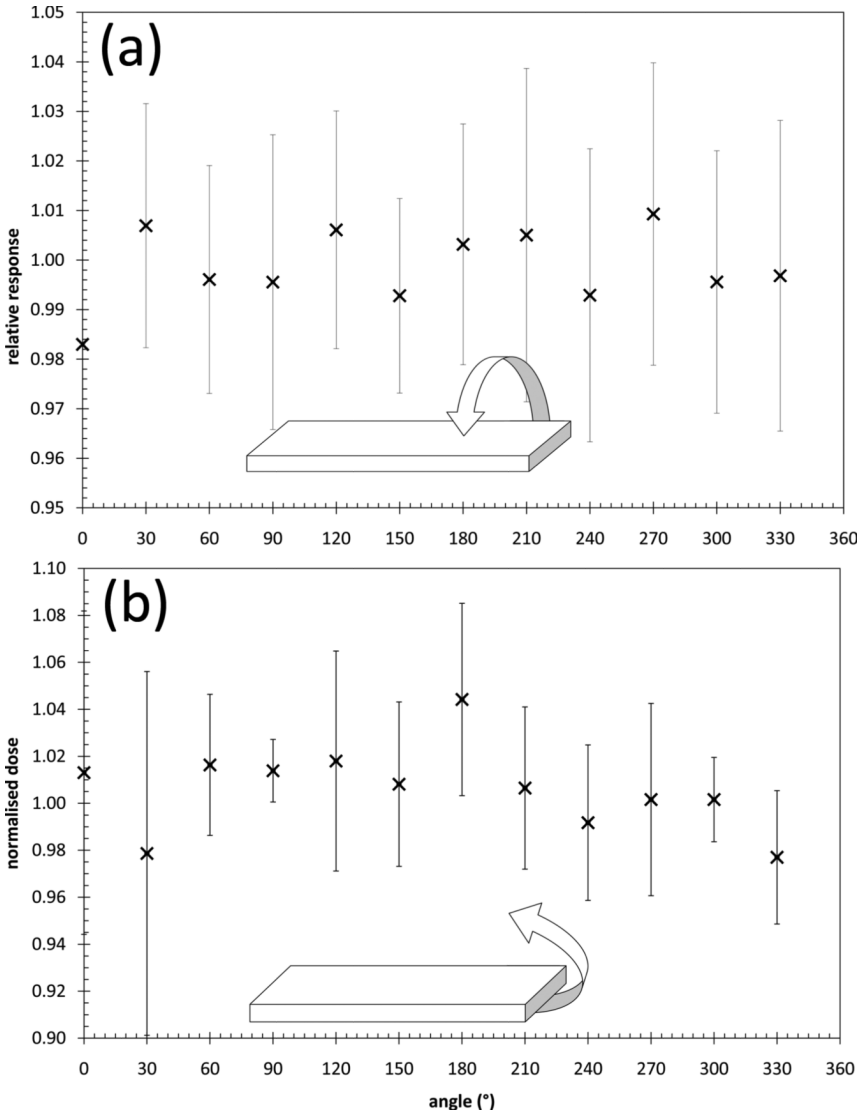

Figure 3.
Angular dependence of the dual MOSFET detector for (a) azimuth and (b) polar axes. The error bars represent two standard deviations of the mean of three measurements.

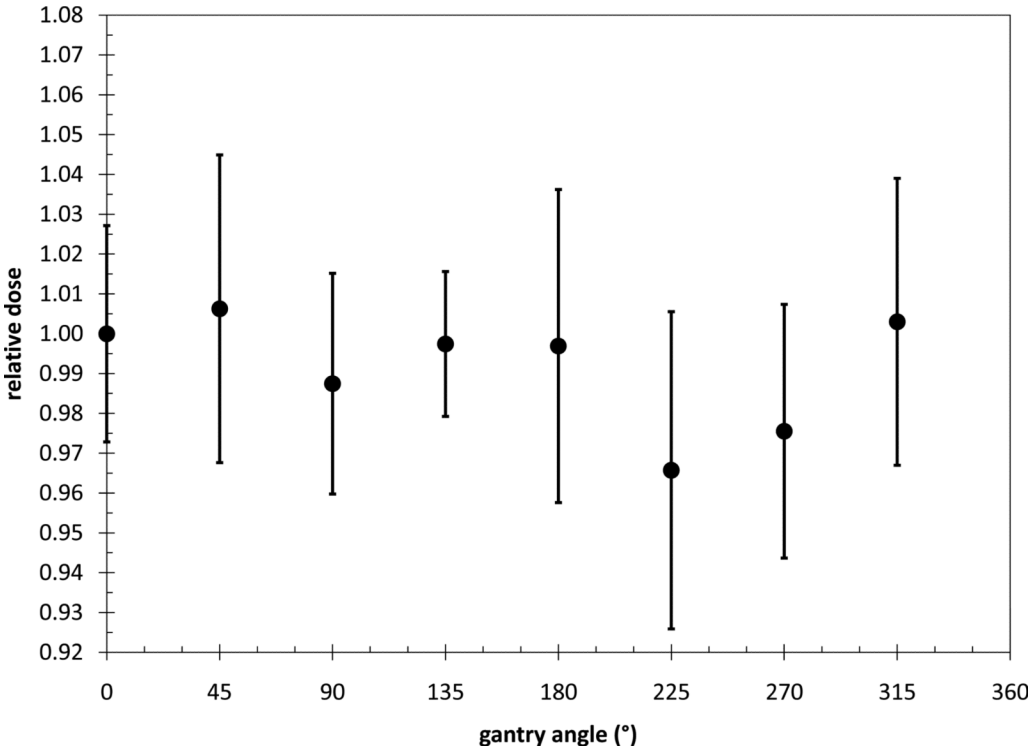

Figure 4.
Dual MOSFET dose relative to Ion Chamber measured dose at the centre of the I'mRT phantom for a range of beam angles. The error bars are two standard deviations of the average of three measurements.

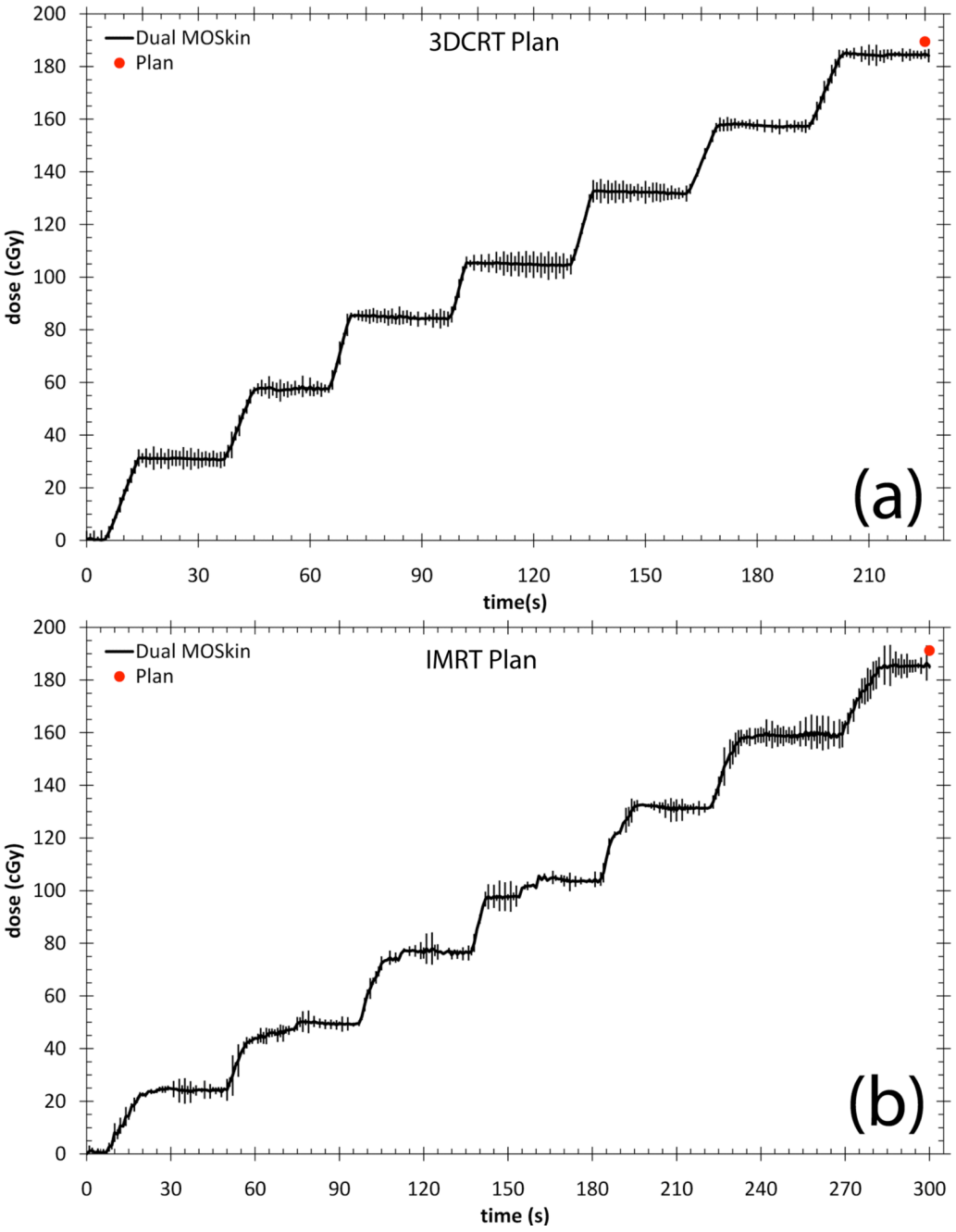

Figure 5.
Real-time measured anterior rectal wall dose for (a) 3DCRT plan and (b) IMRT plan. The error bars are the 95% confidence interval of the average of three measurements.

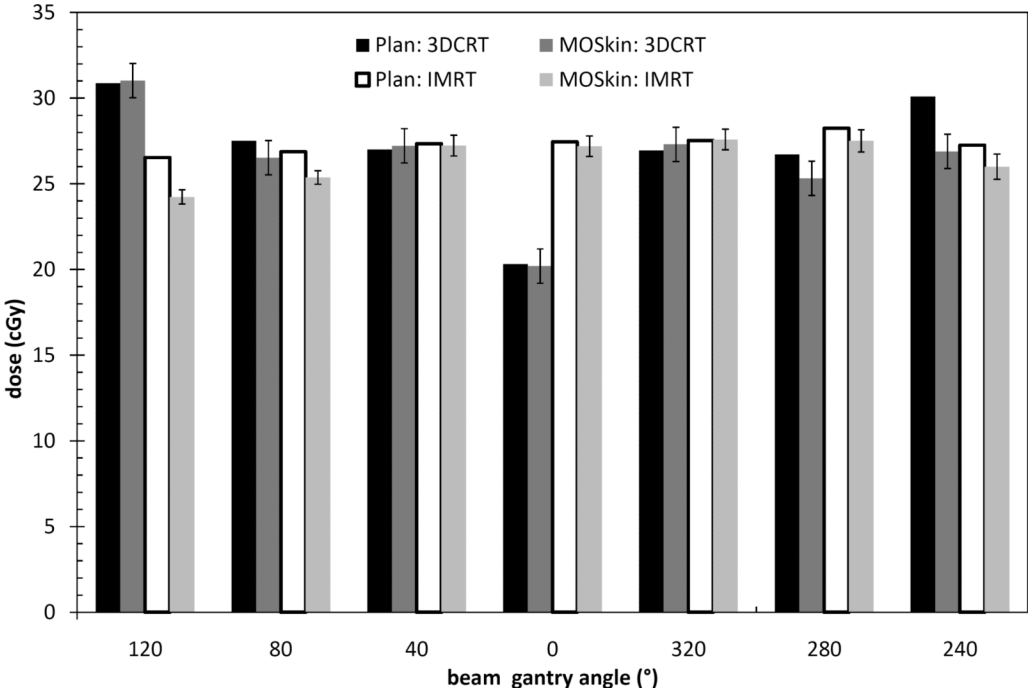

Figure 6.
A field-by-field comparison of the RTPS calculated and MOSFET measured anterior rectal wall dose for the 3DCRT and IMRT deliveries

Table 1

MOSFET sensitivity for varying fraction sizes

Fraction Size (cGy)	Dose per 'beam' (cGy)	Sensitivity (mV/cGy)
203	29	2.63
252	36	2.63
301	43	2.65
350	50	2.65
497	71	2.63
749	107	2.61
1001	143	2.62
	Average (± S.D)	2.63 ± 0.01